Supporting information for:

2D MoS_2/BiOBr van der Waals heterojunctions by liquid-phase exfoliation as photoelectrocatalysts for hydrogen evolution

Mengjiao Wang,[a] Silvio Osella,[b] Rosaria Brescia,[c] Zheming Liu,[d] Jaime Gallego,[a] Mattia Cattelan,[e] Matteo Crisci,[a] Stefano Agnoli[e] and Teresa Gatti[a,f]

[a] Institute of Physical Chemistry and Center for Materials Research (LaMa), Justus Liebig University, 35392 Giessen, Germany

[b] Chemical and Biological Systems Simulation Lab, Centre of New Technologies, University of Warsaw, 02097 Warsaw, Poland

[c] Electron Microscopy Facility, Istituto Italiano di Tecnologia, Via Morego, 30, 16163 Genova, Italy

[d] Nanochemistry Department, Istituto Italiano di Tecnologia, 16163 Genova, Italy

[e] Department of Chemical Sciences, University of Padova, 35131 Padova, Italy

[f] Department of Applied Science and Technology, Politecnico di Torino, 10129 Torino, Italy

Table of Contents

- CV stability test of 1% MoS_2/BiOBr (Fig. S12)
- High-resolution XPS spectra of O1s on (a) 1% MoS_2/BiOBr and (b) 10% MoS_2/BiOBr before PEC HER (Fig. S13)

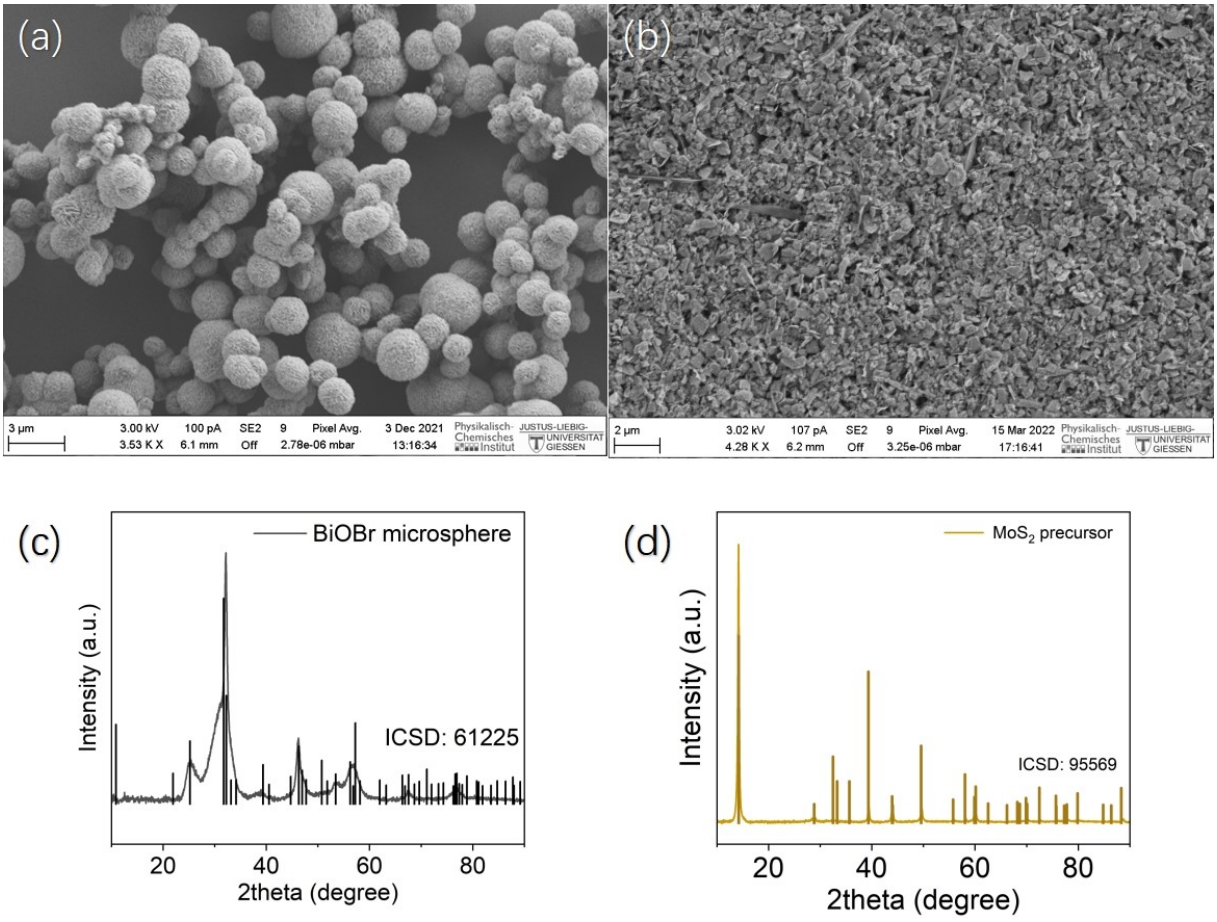

Fig. S1 (a) SEM image and (c) P-XRD of BiOBr microspheres synthesized by solvolthermal method. (b)SEM image and (d) P-XRD of MoS_2 layers. Both materials were used as precursors for the preparation of the HJs.

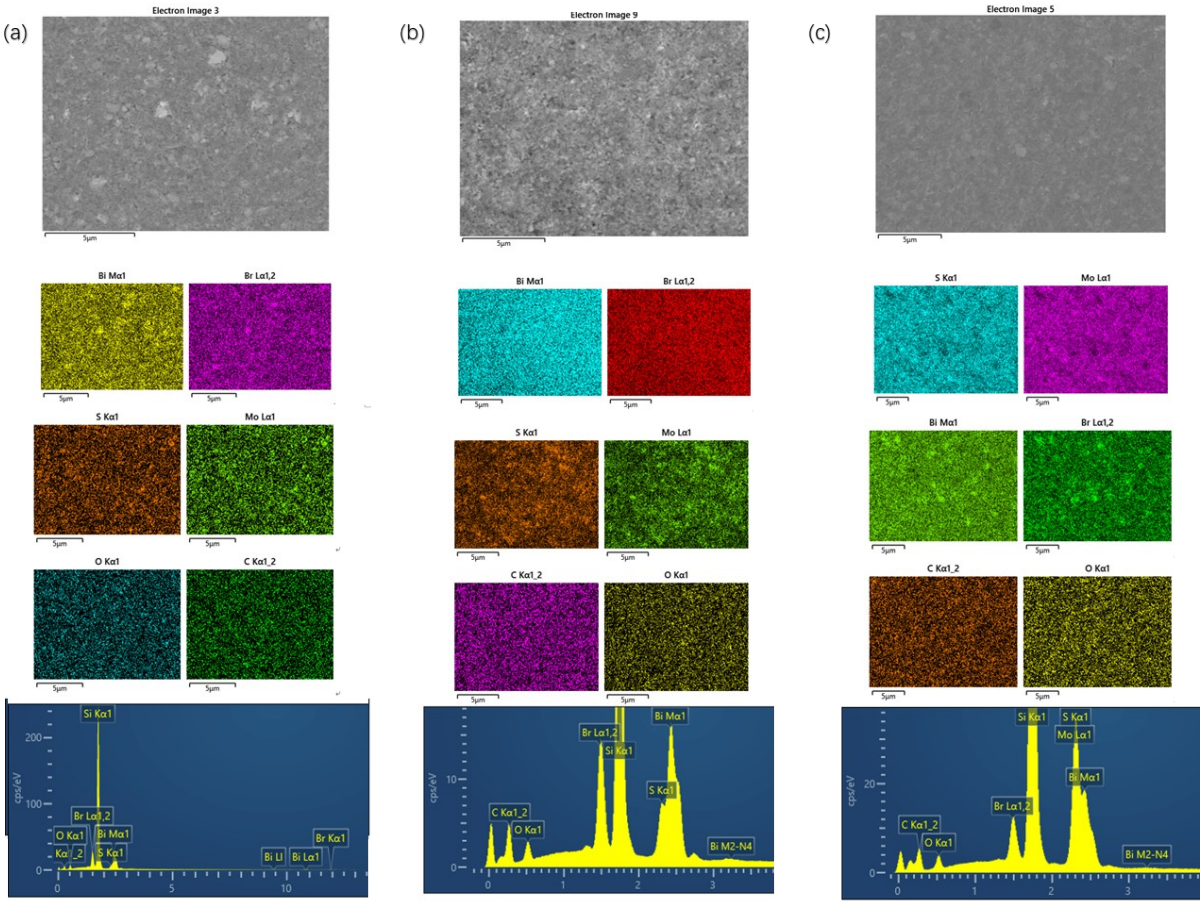

Fig. S2 SEM-EDX elemental mapping and spectra of (a) 5% MoS_2/BiOBr, (b) 10% MoS_2/BiOBr and (c) 50% MoS_2/BiOBr.

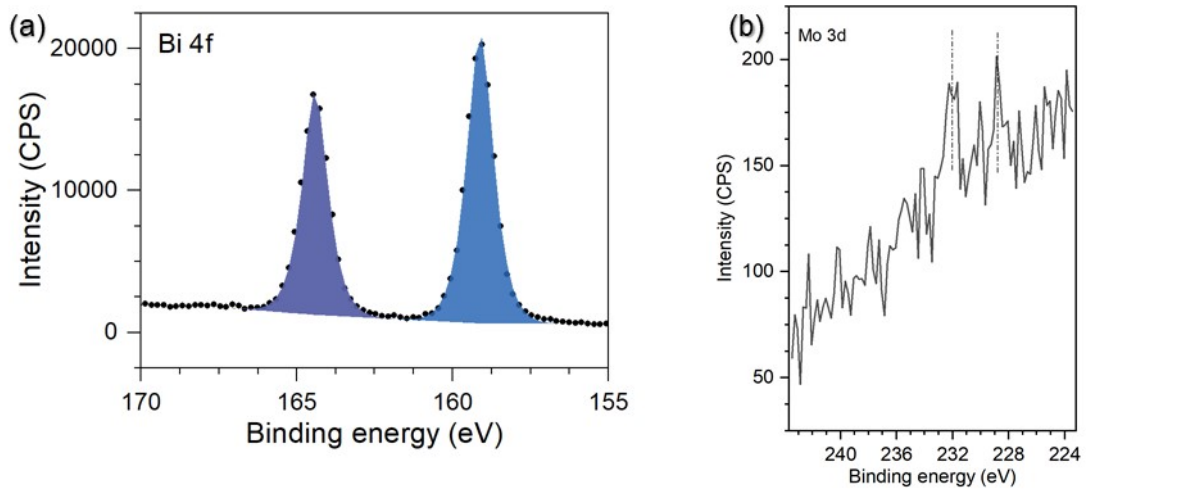

Fig. S3 High resolution XPS spectra of (a) Bi 4f and (b) Mo 3d in 1% MoS_2/BiOBr. Two characteristics peaks around 229.4 and 232.5 eV were observed in the XPS spectrum in Fig. S4, indicating existence of the 2H phase of MoS_2. The weight ratio of MoS_2 is calculated according to the atomic ratio of Mo:Bi.

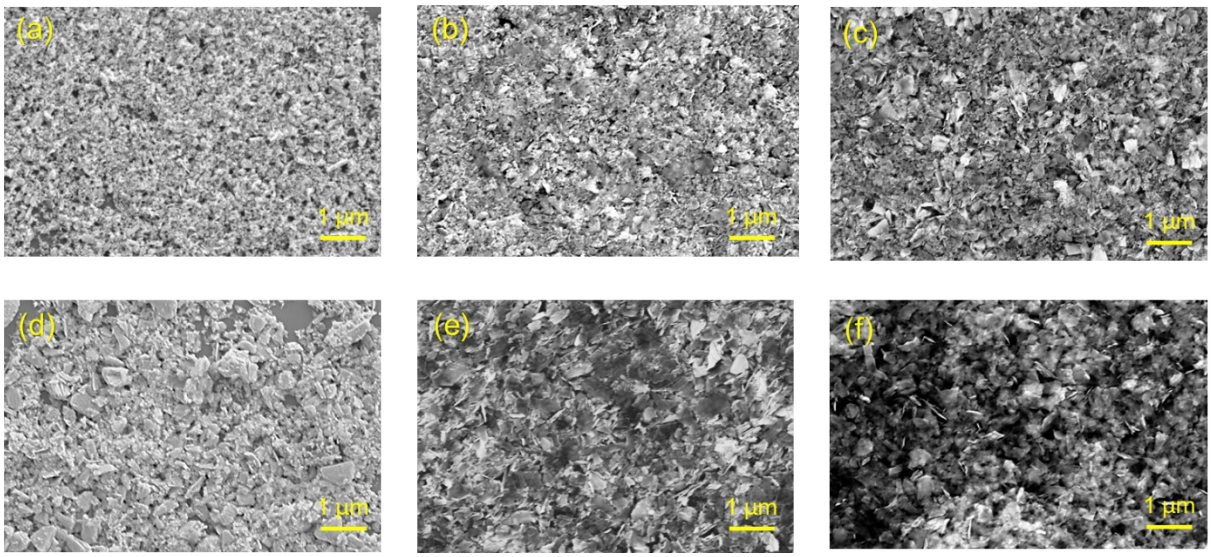

Fig. S4 SEM images of (a) LPE BiOBr, (b) 1% MoS_2/BiOBr, (c) 5% MoS_2/BiOBr, (d) 10% MoS_2/BiOBr, (e) 50% MoS_2/BiOBr and (f) LPE MoS_2.

Table S1 Weights of the precursors used during LPE to synthesize the MoS_2/BiOBr HJs and the same estimated in the resulting materials by XPS and SEM-EDX.

Sample	BiOBr microspheres (mg)	MoS_2 layers (mg)	Ratio calculation	Weight ratio of MoS_2 (%)	Br/Bi atomic ratio	O/Bi atomic ratio
1% MoS_2/BiOBr	200	2.9	XPS	0.9	1.33	1.80
5% MoS_2/BiOBr	200	10	SEM-EDX	4.8	1.32	1.60
10% MoS_2/BiOBr	200	20	SEM-EDX	11.2	1.25	1.20
50% MoS_2/BiOBr	100	100	SEM-EDX	50.2	1.26	2.46

Table S2 Band gap values of the HJs calculated according to the Tauc method.

Sample	Band gap (eV)
2D BiOBr	3.15
1% MoS_2/BiOBr	3.01
5% MoS_2/BiOBr	2.92
10% MoS_2/BiOBr	2.29
50% MoS_2/BiOBr	2.25
2D MoS_2	1.75

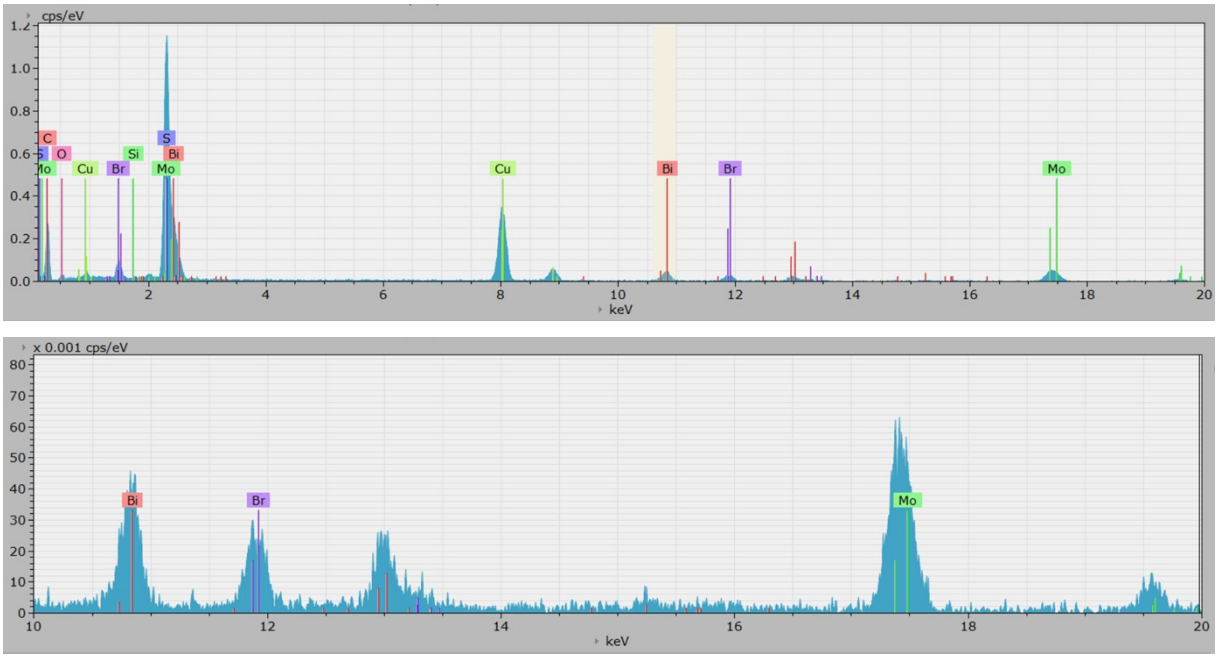

Fig. S5 STEM-EDX spectra corresponding to the map in Fig. 1g) in the manuscript. The elemental maps reported in Fig. 1g) were obtained by integration of the raw spectra, point by point in the image, in the regions corresponding to Bi Lα peak (centered at 10.8 keV) and the Mo Kα peak (centered at 17.5 keV).

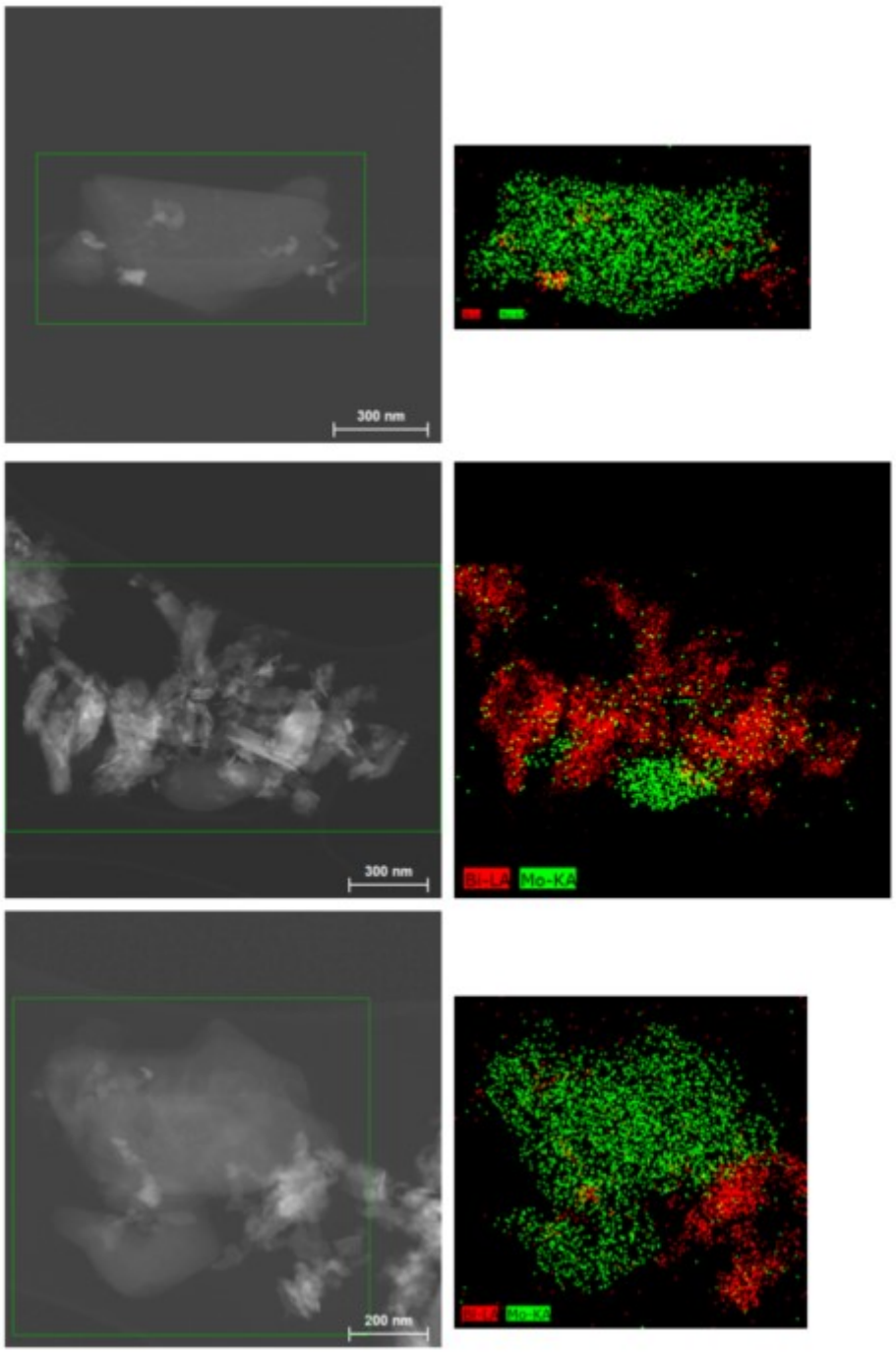

Fig. S6 (left) HAADF-STEM images and (right) corresponding STEM-EDX maps collected on a MoS_2/BiOBr HJ. The comparison between each HAADF-STEM image and the corresponding STEM-EDX map clearly shows a difference in the contrast and morphology of the two components: the MoS_2 flakes are hundreds nanometers extended, lower contrast components, while the BiOBr nanoplatelets are typically less than 100 nm extension and stronger contrast, due to higher atomic number. This image can be correlated with BF-TEM images in Fig. 1b-e in the manuscript, where the MoS_2 flakes appear instead less dark than the BiOBr platelets.

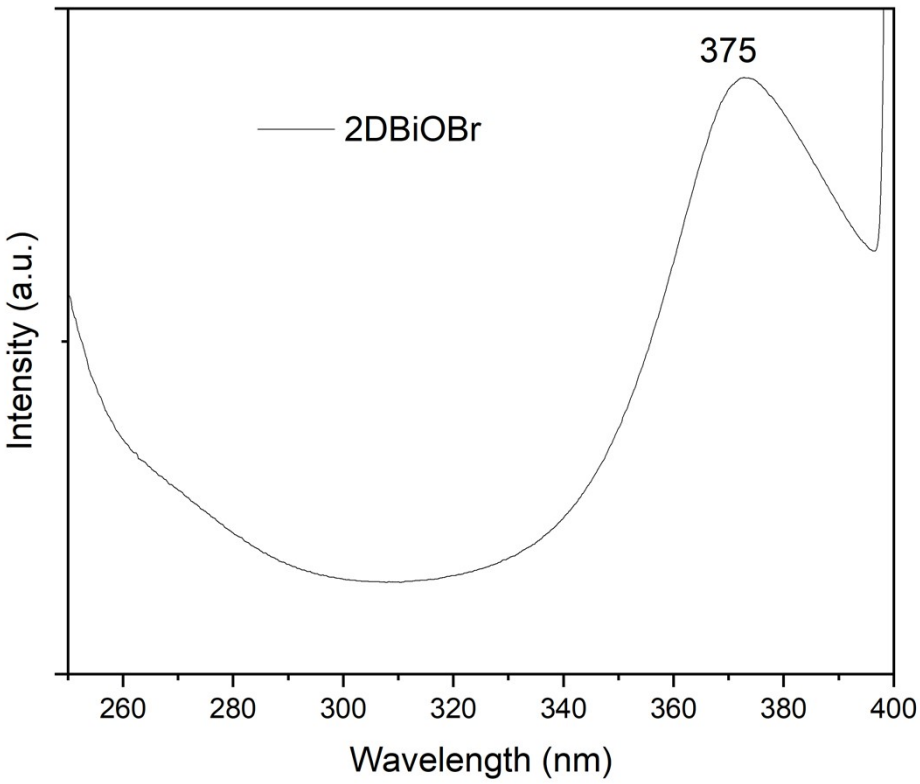

Fig. S7 PL excitation spectrum of 2D BiOBr.

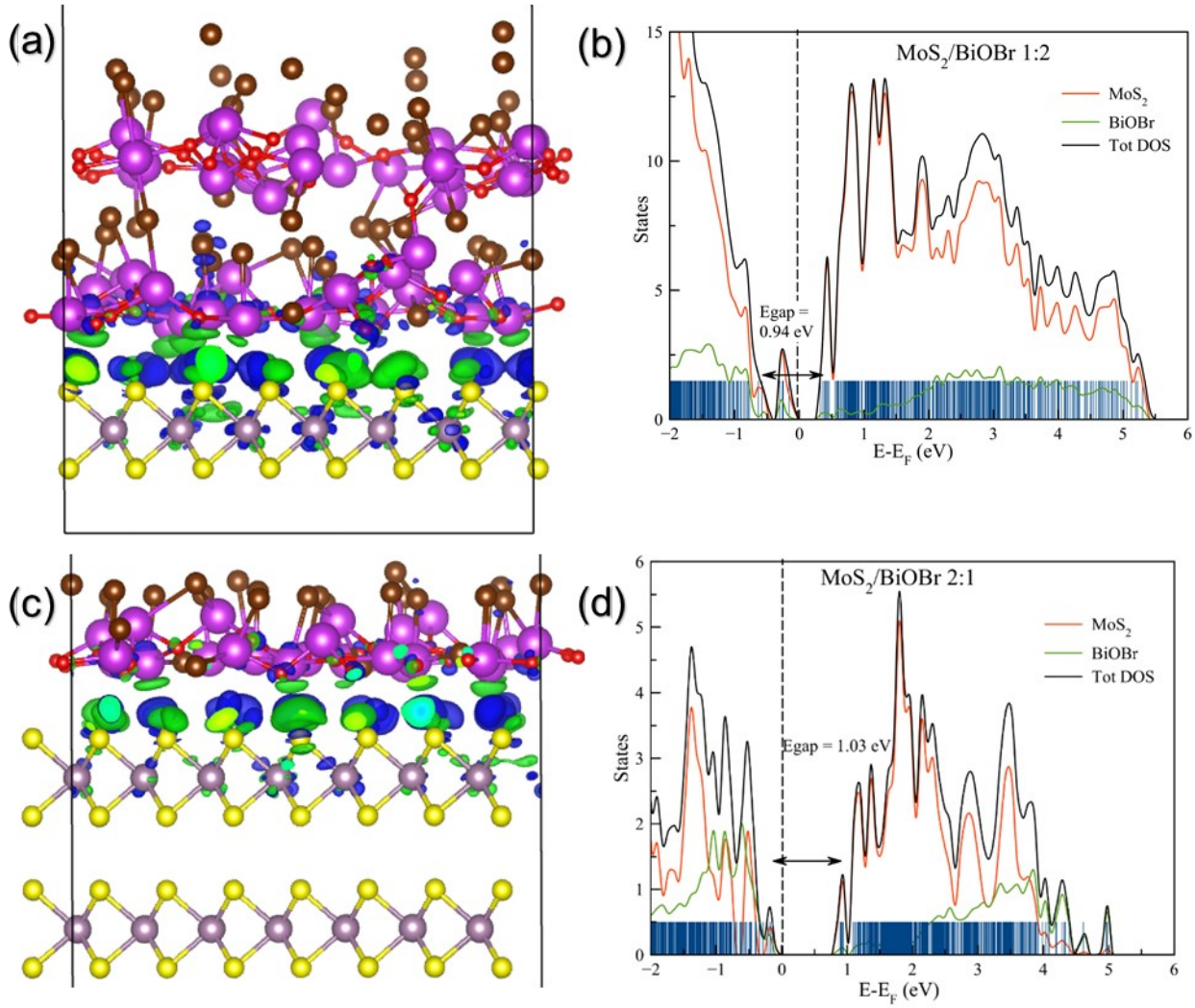

Fig. S8 Optimized structures and charge difference analyses for the three considered interfaces: (a) 1-MoS_2/2-BiOBr and (b) 2-MoS_2/1-BiOBr. The MoS_2/BiOBr interlayer distance is measured in the 0.270-0.292 nm window depending on the number of layers present. The atoms are represented with the following colors; yellow: sulfur, gray: molybdenum, red: oxygen, purple: bismuth, brown: bromine. Blue surface represents negative charge; green surface the positive charge. (c) Total and partial DOS analyses for 1-MoS_2/1-BiOBr and (d) 2-MoS_2/1-BiOBr. The Fermi energy is set to zero (dotted line), blue vertical lines show the eigenvalues of the interface.

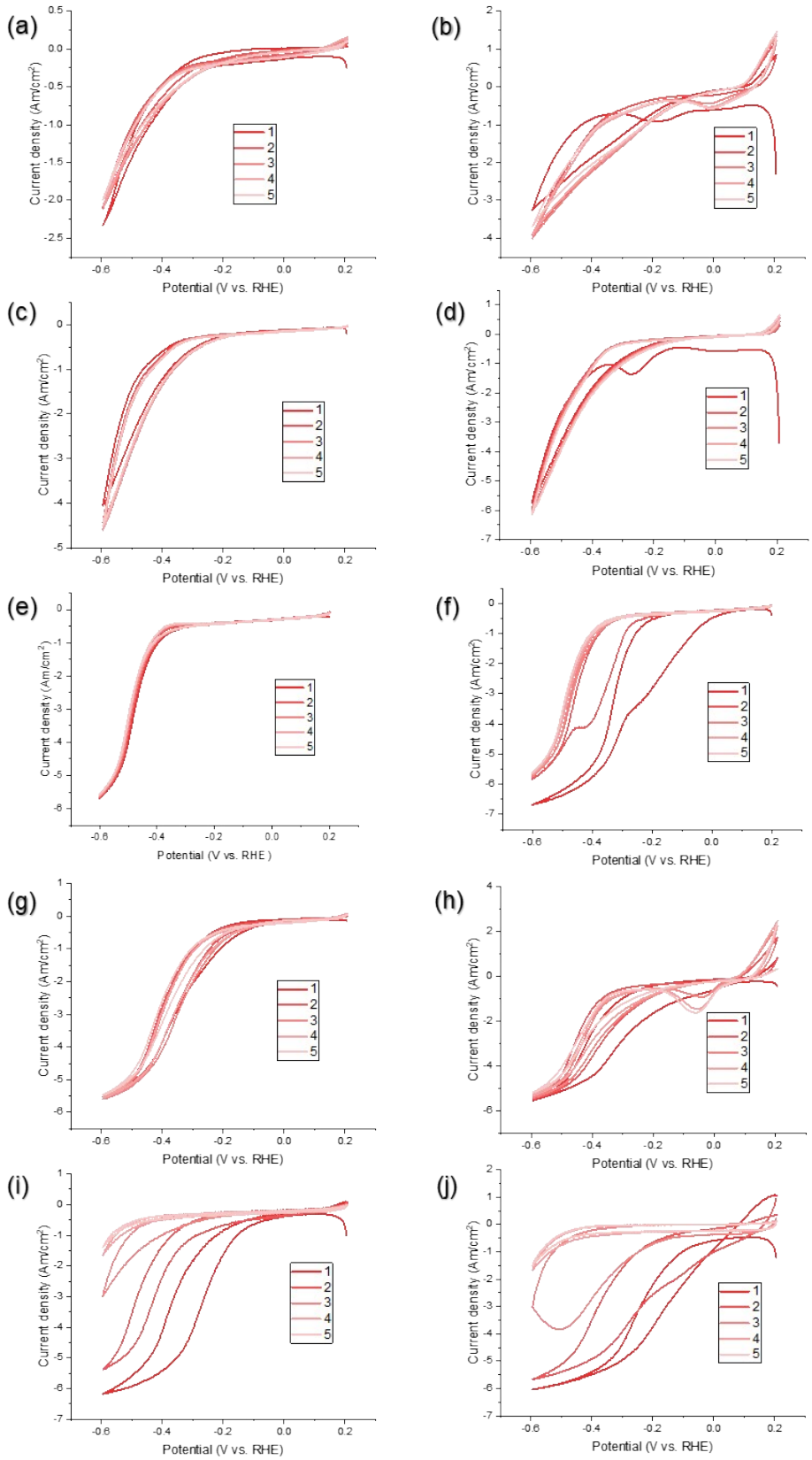

Fig. S9 Cyclic voltammetry curves of 2D BiOBr (a) in the dark and (b) with mercury lamp, 1% MoS_2/BiOBr (c) in the dark and (d) with mercury lamp, 5% MoS_2/BiOBr (e) in the dark and (f) with mercury lamp, 10% MoS_2/BiOBr (g) in the dark and (h) with mercury lamp, 50% MoS_2/BiOBr (i) in the dark and (j) with mercury lamp.

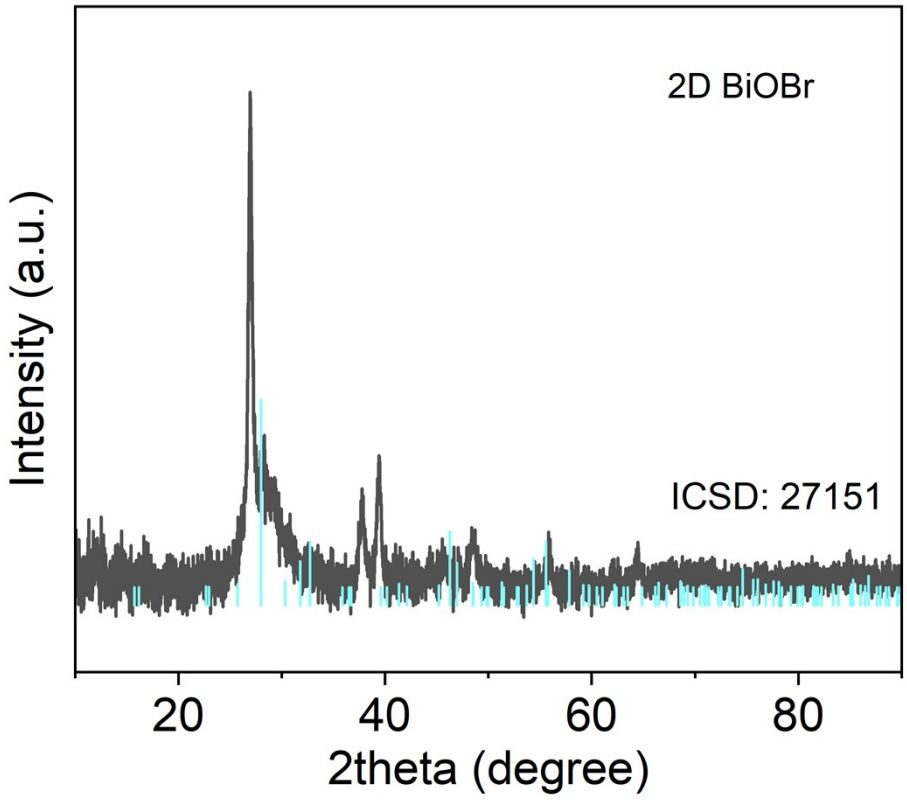

Fig. S10 P-XRD pattern of 2D BiOBr after PEC HER with the reference structure of Bi_2O_3 (ICSD number: 27151).

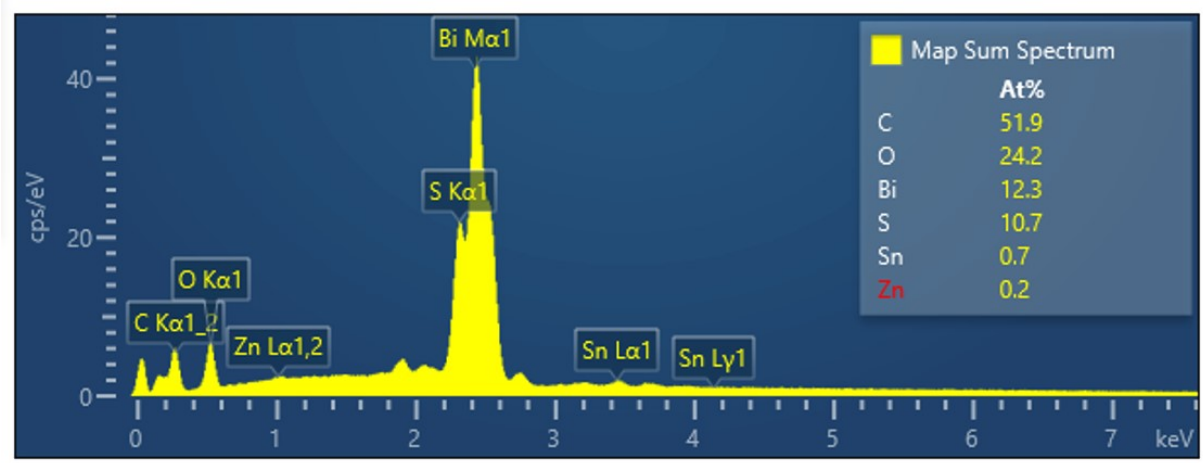

Fig. S11 SEM-EDX spectrum of 10% MoS_2/BiOBr after PEC HER.

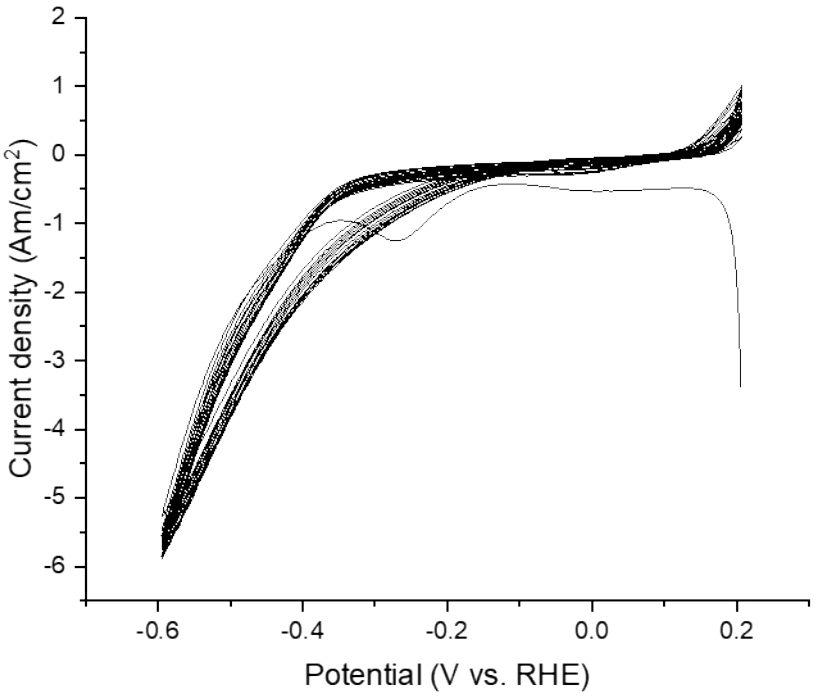

Fig. S12 CV stability test of 1% MoS_2/BiOBr. 16 cycles are shown in the figure.

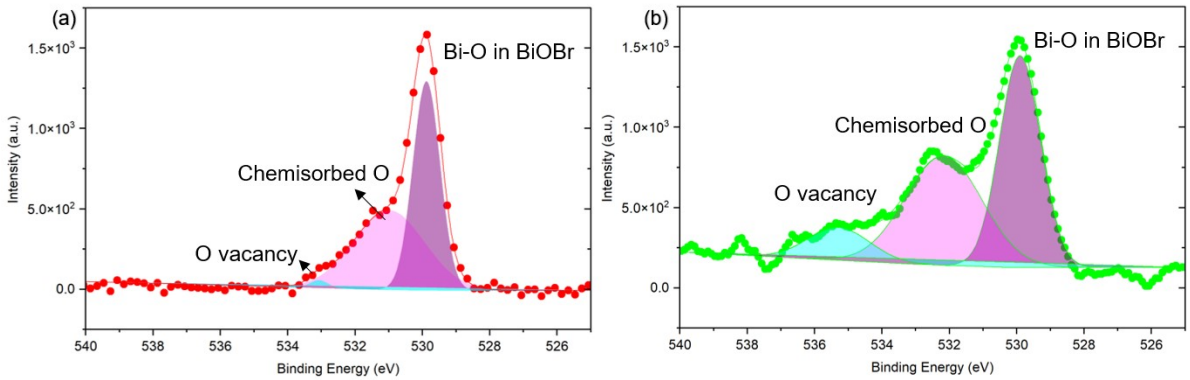

Fig. S13 High-resolution XPS spectra of O1s on (a) 1% MoS_2/BiOBr and (b) 10% MoS_2/BiOBr before PEC HER. In 1% MoS_2/BiOBr, the synergetic effect between MoS_2 and BiOBr enable the preservation of O vacancies (comparison of Fig 6d and Fig S13a). On the contrary, the peak at 535.3 eV indicates that 10% MoS_2/BiOBr contains a large amount of O vacancies before PEC HER. However, the O vacancies are consumed rapidly during PEC HER (comparison of Fig 6d and Fig S13b).